Environmental Science and Pollution Research (2019) 26:9508–9523
https://doi.org/10.1007/s11356-019-04431-8

RESEARCH ARTICLE

Green sol–gel synthesis of novel nanoporous copper aluminosilicate for the eradication of pathogenic microbes in drinking water and wastewater treatment

Bahaa Ahmed Hemdan[1] · Amany Mohamed El Nahrawy[2] · Abdel-Fatah M. Mansour[2] · Ali Belal Abou Hammad[2]

Received: 13 November 2018 / Accepted: 29 January 2019 / Published online: 6 February 2019

Abstract

We used a green sol–gel synthesis method to fabricate a novel nanoporous copper aluminosilicate (CAS) material. Nanoporous CAS was characterized using X-ray powder diffraction (XRD), field emission transmission and scanning electron microscopies (FE-TEM/FE-SEM), Fourier transform infrared (FTIR) spectroscopy, and optical analyses. The CAS was also evaluated for use as a promising disinfectant for the inactivation of waterborne pathogens. The antimicrobial action and minimum inhibitory concentration (MIC) of this CAS disinfectant were determined against eight microorganisms (*Escherichia coli*, *Salmonella enterica*, *Pseudomonas aeruginosa*, *Listeria monocytogenes*, *Staphylococcus aureus*, *Enterococcus faecalis*, *Candida albicans*, and *Aspergillus niger*). An antimicrobial susceptibility testing of CAS was measured. Results of disc diffusion method pointed out that the diameters of the zone using well diffusion were wider than disc diffusion methods, and the findings also showed that the MIC of the CAS disinfectant against *E. coli*, *S. enterica*, and *P. aeruginosa* was 100 mg/L within 20 min of contact time. Meanwhile, the MIC of the CAS disinfectant was 100 mg/L within 40 min of contact time for the other strains. The efficacy of antimicrobial action (100%) reached within 20 to 40 min against all tested microbes. Herein, the antimicrobial susceptibility testing of CAS disinfectant showed no toxicity for human and bacterial cells. It can be concluded that nanoporous CAS is a promising, economically, and worthy weapon for water disinfection.

Keywords Green sol–gel · Nanoporous CAS · Pathogenic microbes · Disinfection · Water purification

Introduction

Water is a vital issue for life on Earth and is a precious resource for human civilization (WHO 2012). The contamination of water resources with waterborne pathogens has garnered great attention and it is leading to the deterioration of water quality worldwide (Pandey et al. 2014). The discharges of raw and poorly treated sewage directly into surface water such as ponds, lakes, and rivers and indirectly to ground water through percolation are also considerable sources of fecal contamination containing many kinds of enteric pathogenic microbes. These wastes also contain large concentrations of some enteric bacterial species, including *E. coli, Salmonella* spp., *Vibrio* spp., and *Shigella* spp., that can cause illnesses in humans, such as severe fever, cholera, and diarrhea, particularly in developing countries (Pandey et al. 2014). Furthermore, the presence of these pathogenic microbes is a serious concern for nearly all types of surrounding aquatic environments, making it essential to understand their effects (United States Environmental Protection Agency 2017). Similarly, many outbreaks, particularly in low-income countries, could occur due to the contamination of drinking water by diverse types of pathogenic microbes, including bacteria, viruses, and protozoa. These pathogens can infect millions of inhabitants, such as infants, pregnant women, and people with a low immunity level (Craun et al. 2006; Fenwick 2006). In addition, intestinal cases related to drinking water are not reported carefully, even in advanced nations, because of

Responsible editor: Angeles Blanco

✉ Bahaa Ahmed Hemdan
bahaa_nrc@yahoo.com

[1] Water Pollution Research Department, Environmental Research Division, National Research Centre, 33 El-Bohouth St., Dokki, Giza 12622, Egypt

[2] Solid-State Physics Department, Physics Research Division, National Research Centre, 33 El-Bohouth St., Dokki, Giza 12622, Egypt

inaccuracies in the observations and in studies of infectious diseases (Ford 1999; Hellard et al. 2001). In the USA (with roughly 300 million people), 12–19 million gastric cases related to contaminated drinking water have been reported annually (Reynolds et al. 2008). Likewise, the World Health Organization (WHO) revealed that water-related diseases have resulted in the death of 3.4 million people (mainly children) each year (World Health Organization; UN-Water 2014). In addition, the United Nations Children's Fund (UNICEF) stated that 4000 children die daily as a consequence of untreated and polluted water (UNICEF 2014).

Contaminated water can be purified using classical disinfectants. Among these disinfectants, chlorine is a potent oxidant that can effectively eradicate waterborne pathogens. Chlorine is the most frequently used disinfectant for water treatment and has an extensive spectrum of antimicrobial action; however, carcinogenic and hazardous by-products such as haloacetic acids (HAAs) and trihalomethanes (THMs) can be produced when chlorine reacts with organic materials (Simões et al. 2010; Sedlak and Von Gunten 2011; Jamil et al. 2015). These carcinogenic compounds show severe toxicity to humans and can cause potential public health problems (Zazouli and Kalankesh 2017). Although solar radiation, UV disinfectants, and photocatalytic oxidation have been used for the inactivation and destruction of pathogenic microbes, these disinfectants have some limitations, including high energy intensity, inconvenience, and high costs (Hisatomi et al. 2014; Trojanowicz et al. 2018).

Currently, nanoscale particles have been recognized as a novel and promising approach to solve much more difficult problems due to their outstanding bactericidal effects. Numerous investigations have also carefully studied these nanoparticles (NPs) with metal and/or metal oxides for their antimicrobial action against many types of pathogenic microorganisms (Khezerlou et al. 2018). Magnetic thiourea-formaldehyde polymer (MTUF) nanoparticles have a good ability to remove Gram-negative and Gram-positive bacteria and *Candida albican* from water samples (Elwakeel et al. 2018).

In recent decades, the development of inorganic porous nanomaterials has progressed rapidly because these materials can be formed in two phases: crystalline and amorphous. The formation of an open structure with a high surface area strengthens the abilities of nanoporous materials in various applications, such as catalysis, ion exchange, optoelectronics, adsorbents, energy storage materials, environmental engineering materials, and advanced nanotechnology. Many novel nano-sized materials with preferred structures, morphologies, and properties have been developed. The different inorganic nanoporous materials include natural zeolites, silica-based porous or microporous materials, different oxides (GeO_2, $AlPO_4$, etc.), and even organic-inorganic hybrid materials (Guo et al. 2013; El Nahrawy et al. 2016; Bian et al. 2018).

To date, silica-based materials have been extensively used in scientific and industrial applications such as lenses, optics, food packaging, electronic devices, and automobile parts, as well as in many biotechnology applications (drug delivery, bone composites, and dental composites), due to their cost-effectiveness, excellent thermal stability, high chemical stability, and environmental friendliness (Jin et al. 2014; Zhan et al. 2015; El Nahrawy et al. 2018).

The fabrication of silica-based materials modified with different particles possessing controllable nanostructures has become more attractive than the synthesis of solid phase particles because of the new prospective applications and their enhanced performance (Youssef et al. 2017; Wang et al. 2018). Among the silica-based materials, copper aluminosilicate (CAS) has gained attention due to its nanoporous structure, high specific surface area, and excellent optical properties, making it potentially useful for different applications (De Velasco-Maldonado et al. 2018; Alghamdi et al. 2018). Thus, the present study was conducted to (i) improve the facile sol–gel and green synthesis of CAS NPs for optical applications and (ii) apply the synthesized CAS NPs as a promising and economical disinfectant for the eradication of waterborne pathogens during water and wastewater treatment.

Experimental

Synthesis of nanoporous copper aluminosilicate using a green acidic sol–gel method

Nanocrystalline copper aluminosilicate (CAS) (10 Cu_2O_3: 25 Al_2O_3: 65 SiO_2) was synthesized by a modified sol–gel method. First, a silica-based material was prepared using the well-established acidic sol–gel method at room temperature (i.e., 26 ± 1 °C) (El Nahrawy and Ali 2014). The sol of the silica system was composed of the precursor (tetraethyl orthosilicate $(C_2H_5O)_4Si$ (TEOS, 99.999%, Sigma-Aldrich), which was added to absolute ethanol (EtOH)/distilled water and a dilute hydrochloric acid solution. The mixture was allowed to hydrolyze for 1 h under magnetic stirring to form a clear and homogeneous silica sol as a base. In similar steps, the required amounts of aluminum and copper nitrate were dissolved in absolute ethanol/distilled water, and hydrochloric acid was added as the catalyst under continuous magnetic stirring for 1 h. Silica sol was collected as a green transparent solution at 40 °C for another 2 h. The pH value of the solution was regulated to 9 by adding ethylenediamine. Then, the produced homogeneous sol of CAS was transferred into a glass container and kept for 1 week at 50 °C for gelation. Then, the wet nanogel was dried for 48 h at 200 °C and before heat treatment at 850 °C for 4 h.

Characterization studies of the pure and doped nanoporous CAS disinfectant

X-ray powder diffraction (XRD) patterns were obtained on a Bruker D8 Advance diffractometer using CuKα radiation (λ = 1.540 Å), operating at 40 kV and 40 mA. Scans were performed with a detector step size of 0.0200B0over an angular range of 2θ starting from 10 to 80°. The surface morphology of the as-prepared samples was investigated using field emission scanning electron microscopy (FE-SEM) (JEM-1230). Samples were coated with gold at 10 mA for 2 min prior to SEM analysis. The chemistry of the prepared nanocrystalline CAS was analyzed using Fourier transform infrared (FTIR) spectrometry (Nicolet Magma550 series II, Midac, USA) at wavelengths ranging from 4000 to 400 cm^{-1} using the disc method. The particle size and distribution of the nanoporous sample were determined by high-resolution transmission electron microscopy (HR-TEM) (JEM-2100, Jeol, Japan). The surface morphology of the nanoporous sample was characterized by FE-SEM (QUANTA-250, Japan).

Optical measurements

To check the optical benefits of nanoporous CAS, the absorption coefficient and refractive index were evaluated as a function of changes in wavelength. The optical direct transmittance and reflectance were evaluated at a vertical light incidence throughout the spectral limit of 190–2500 nm. The film transmittance and reflectance spectra were captured via a JASCO double beam spectrophotometer (model V-570 UV-Vis-NIR). The measurements were established at ambient temperature. The optical features were estimated from the absolute amounts of total experimental transmittance T_{msd} and reflectance R_{msd} subsequent to making modifications attributable to the substrate absorbance and reflectance. The absolute value of T_{msd} was calculated as follows (Farag et al. 2012):

$$T = Tmsd(1-Rquz) \quad (1)$$

The absolute value of R_{msd} was computed as follows:

$$R = R_{msd}R_{Alum}\left[\left(1-R_{quz}\right)^2 + 1\right] - T^2R_{quz} \quad (2)$$

where R_{quz} and R_{Alum} are the reflectances of the reference quartz substrate and that of the reference aluminum mirror, respectively.

Preparation of disinfectant

The stock solution nanoporous CAS disinfectant was prepared by adding 1 g of disinfectant in 10 mL sterile distilled water. Then, the prepared stock solution was filtered using a disposable filter with a pore size of 0.22 μm. Three different doses of CAS disinfectant (25, 50, and 100 μL) were assessed against potential microbial pathogens.

Microorganisms used

The potential microbial strains used in this study were as follows: *Escherichia coli* ATCC 25922, *Salmonella enteric* serovar *typhimurium* ATCC 14028, *Pseudomonas aeruginosa* ATCC 10145, representing Gram-negative bacteria; *Listeria monocytogenes* ATCC 25152, *Staphylococcus aureus* ATCC 43300, and *Enterococcus faecalis* ATCC 43845, representing Gram-positive bacteria; *Candida albicans*, representing yeast; and *Aspergillus niger* local strains, representing fungi.

Antimicrobial effect of nanoporous CAS against microbial pathogens

Well and disc diffusion methods

The use of nanoporous CAS disinfectant agents against some tested potentially pathogenic microorganisms was evaluated using agar dilution methods (well and disc diffusion) (PA 2015).

Determination of minimum inhibitory concentrations

The minimum inhibitory concentrations (MICs) of the nanoporous CAS disinfectant were examined against the mentioned potential microbial pathogens (Zhang et al. 2004). The numbers of viable cells for tested potential pathogenic microorganisms after exposure to the disinfectant were counted using the pour plate method. All experiments were performed in triplicate and repeated at least twice on different days (American Public Health Association et al. 2012).

Kinetic measurement of the bacterial growth curve

To assess the growth curve of the tested bacterial strains, the absorbance (OD) of each bacterial culture containing the nanoporous CAS disinfectant was measured using a spectrophotometer (Cary 100 UV-Vis, Agilent, USA) at 600 nm within 24 h. Samples were taken in 30 min intervals (Jones 1973).

Toxicity assay

Toxicity tests of nanoporous CAS disinfectant agents were performed using both a Microtox Analyzer 500 and cytotoxicity methods on the Hep-2 cell line (Hao et al. 1995; Elith and Leathwick 2009).

Investigation of CAS disinfectant for water disinfection

Three different types of water (Raw Nile water, drinking water inoculated with tested pathogens, and raw domestic wastewater) were disinfected with the effective dose of studied CAS disinfectant agent. *E.coli*, *S. enterica*, *P. aeruginosa L. monocytogenes*, *S. aureus*, *E. faecalis*, *C. albicans*, and *A. niger* were determined in the tested water samples before and after disinfectant treatment by plating onto rapid HiColiform agar, Improved Salmonella agar, Hifluoro Pseudomonas agar Hicrome Aureus agar, Hicrom Listeria selective agar, Hicrome Enterococcus agar, Hicrome Candida agar, and Fungal agar, respectively. All the used chromogenic media were purchased from HiMedia Co., India (American Public Health Association et al. 2012).

The effective dosage of CAS disinfectant was added onto three flasks each one containing 50 mL of raw Nile water, inoculated drinking water, and the influent wastewater samples for disinfection. The flasks were stirred at 250 rpm and ambient temperature. The potential microbial pathogens were enumerated within different time intervals as follows: 0, 15, 30, 45, 60, 120 min and after 24 h, and proper volume (100 μL) from each flask were streaked onto the surface of mentioned chromomeric agar medium. Then, all inoculated plates were incubated at 37 °C for 24 h for bacterial growth and at 30 °C for 48–72 h for fungal growth and suspected colonies were enumerated using colony counter. All of the experiments were repeated three times (Elwakeel et al. 2018).

Results and discussion

Phase purity (XRD)

The recorded XRD pattern after the calcination of the nanoporous CAS sample at a low temperature of 850 °C is shown in Fig. 1. The discernible peaks confirmed the formation of nanoporous CAS, indicating the formation of very fine crystallites. During the phase transformations, the Cu:Al:Si nanogel-to nanopowder was simultaneously cross-linked to form CAS at a low temperature of 200 °C, and the lack of (OH) hydroxyls and EtOH caused more space to be occupied between the forming monomers, which prevents the reaction between hydroxyls and EtOH groups (Øye et al. 2006; El Nahrawy and Ali 2014).

Additionally, the synthesized nanopore structure of CAS resembles the ordering and rearrangement of liquid-crystalline phases where H_2O and EtOH are replaced by the copper-aluminum-silica framework during the densification process. Therefore, calcination at 850 °C appeared to form the dominant crystalline structure, with sharp diffraction peaks attributed to the ($Cu_{5.68}Al_{12}Si_{12}O_{48}$) cubic nanoporous CAS disinfectant. The calculated crystallite size for CAS NPs is 23 nm, which is estimated by Scherrer's formula (El Nahrawy 2015).

HR-TEM and FE-SEM

To better understand the NP distribution and surface morphology, the synthesized sample was characterized by HR-TEM and FE-SEM, as shown in Fig. 2a, b. The TEM image of CAS prepared through the acidic sol–gel process shows the synthesized nanospheres, which were highly clustered and agglomerated, as indicated in the black region in the image in Fig. 2a.

The clustering of CAS nanoporous structures is concomitant with the generation of a highly crystalline structure, confirming the exclusive formation of CAS nanocrystallites. Nanospherical and more dispersed fine nanoparticles are observed in the image, and this might be attributed to the high content of the H_2O/ethanol mixture that accelerates the incorporation of copper and aluminum into silica precursors during the hydrolysis mechanism. This behavior promotes the synthesis of Si–O–Al–OH, Si–O–Cu– OH, Si–O–Al and the direct synthesis of (Si–O–Si), which generates more

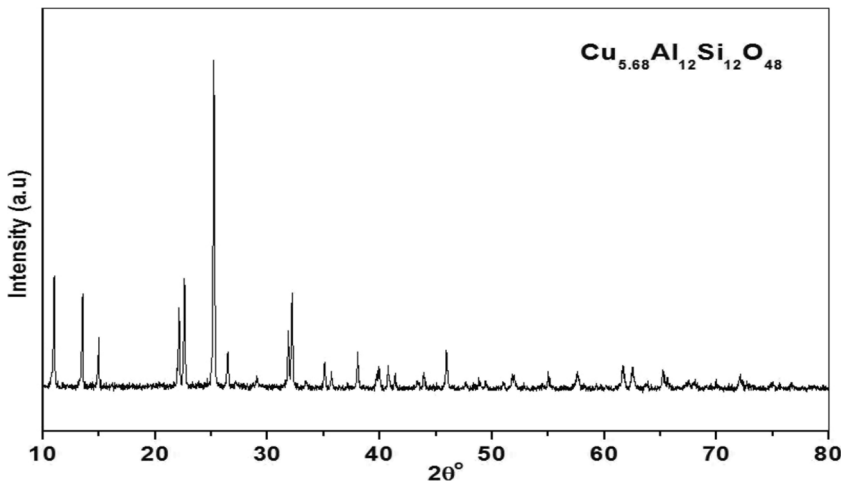

Fig. 1 XRD pattern of the synthesized nanoporous CAS disinfectant, calcined at 850 °C

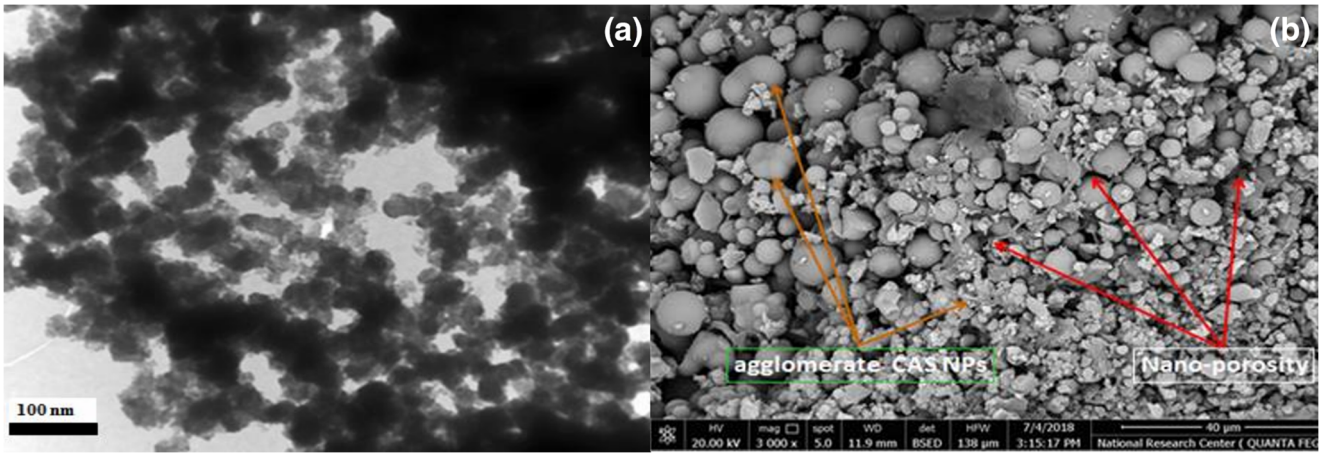

Fig. 2 **a** HR-TEM and **b** FE-SEM of the synthesized CAS nanoporous, calcined at 850 °C

nanospheres and extra NPs during the sol–gel aging polycondensation process (Tripathi et al. 2006).

As shown in Fig. 2b, the surface of the structure contained nanospheres of different sizes and exhibited a highly nanoporous structure. This confirmed the existence of the strong interaction and strong cross-linkage between the silica, alumina, and copper NPs in the nanoporous CAS disinfectant.

FTIR spectrum

The FTIR spectrum of the nanoporous CAS calcined at 850 °C in the range of 4000–400 cm^{-1} is presented in Fig. 3. The characteristic broad band at 3451 cm^{-1} was ascribed to hydroxyl groups (–OH) and the stretching vibration of silanols (El Nahrawy et al. 2016; El Nahrawy and AbouHammad 2016). These (–OH) groups mainly originate from Si–O–OH, Al–O–OH, and Cu–O–OH vibrations in the CAS networks (Hongquan et al. 2003). The distinct band at ~ 1639 cm^{-1} corresponds to the (OH) bending vibration mode of adsorbed OH groups (Kajihara 2013). The highest intensity band at 1096 cm^{-1} was ascribed to the stretching mode of (Si–O–Si), (Si–O–Al), and (Si–O–Cu), while the absorption band at 971 cm^{-1} was attributed to the asymmetric stretching mode of Si–O–Al, Si–O–Cu, and Si–O–OH (Kaur et al. 2018). The characteristic bands in the lower wavenumber region of 971 to 469 cm^{-1} are ascribed to the vibration bands of Si−O−M (M=Si, Al, and Cu) and the symmetric stretching (bond rocking) of Si−O−Si (Kaur et al. 2016). The occurrences of these bands at 1100–469 cm^{-1} suggest the generation of highly crystalline CAS (Kaur et al. 2016).

Optical properties of nanoporous CAS

To identify their absorption coefficient and refractive index, CAS NPs were examined using spectral transmittance and reflectance experiments. The spectral allocation of the transmittance and reflectance for the prepared nanoporous CAS is displayed in Fig. 4a-d. The transmittance curve of the nanoporous sample increases rapidly from 260 to 300 nm, expressing a fundamental transmittance edge. The sample

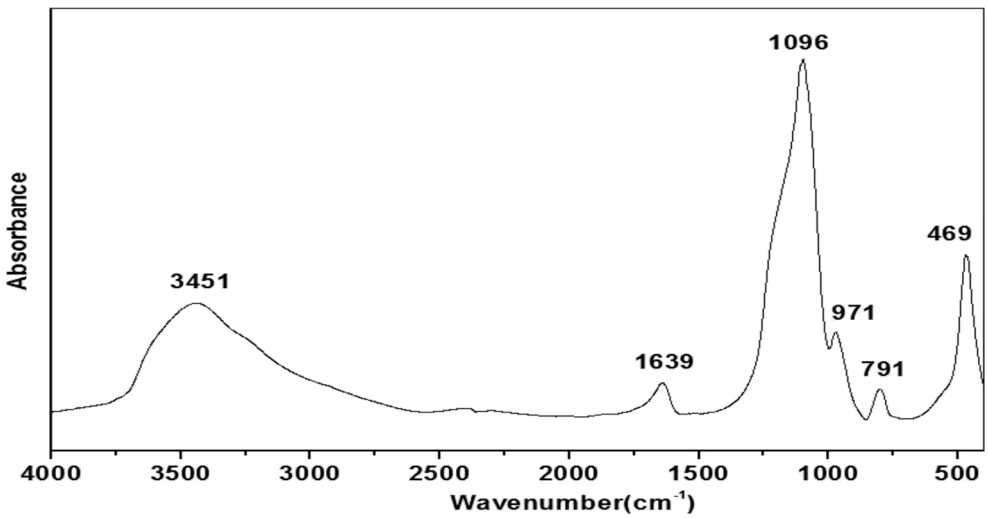

Fig. 3 FTIR of the synthesized CAS nanoporous, calcined at 850 °C

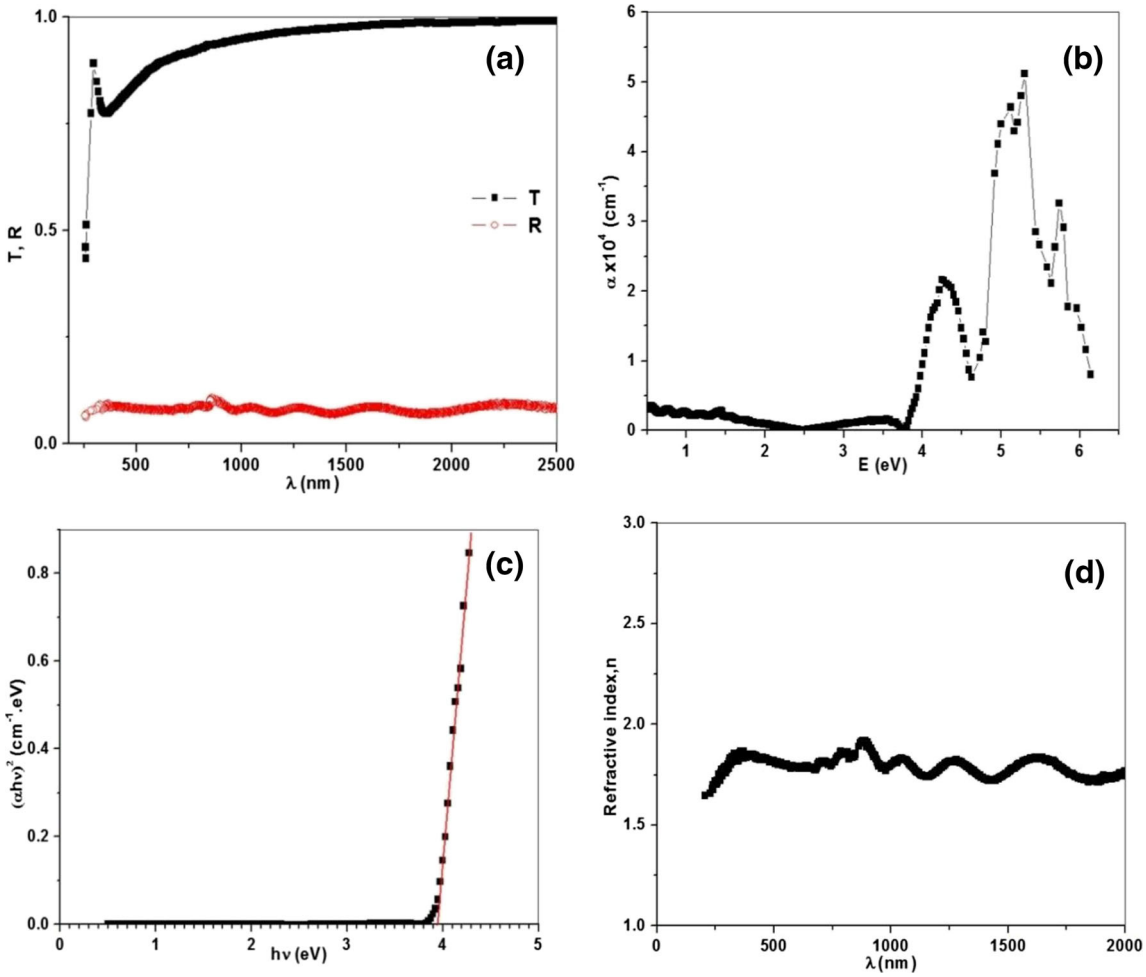

Fig. 4 **a** The optical transmittance and reflectance. **b** The absorption coefficient. **c** Tauc's plot. **d** The refractive index for the CAS nanoporous, calcined at 850 °C

displays a second edge beyond the transmittance range of 360–580 nm, as shown in Fig. 4a. Over this range, the transmittance intensity increases slightly with increasing wavelength. The reflectance curve of the nanoporous CAS is almost unchanged with increasing wavelength. In general, at wavelengths below 580 nm, the sample is absorbing light, while at wavelengths over this value, the prepared sample is transparent.

The optical absorption coefficient (α) of the nanoporous CAS disinfectant explains the absorption operation in several photon energy values, as shown in Fig. 4b. This approach is employed to identify the characteristics of electronic integrand transitions and to measure the optical band gap of non-metallic materials. The transmittance and reflectance values were utilized for the computation of the absorption coefficient (α) employing the following formula:

$$\alpha = (1/t)\, ln\left(\left((1-R)^2/2T\right) + \sqrt{\left[\frac{(1-R)^4}{4T^2}\right] + R^2}\right) \quad (3)$$

where t is the film thickness.

The absorption coefficient (α) for the nanoporous CAS is shown in Fig. 4c. At the lower energy values below 3.8 eV, the absorption coefficient is small. This value increases as the optical energy increases, showing four highly intense absorption bands at 4.25, 5.13, 5.31, and 5.76 eV. The absorption edge is employed to find the band gaps of the nanoporous CAS with Tauc's approach (Mansour et al. 2017a):

$$\alpha = \frac{p}{h\nu}\left(h\nu - E_g\right)^b \quad (4)$$

where p is a variable determined by the transition possibility and E_g is the optical band gap. In this formula, the exponent b is considered to be equal to (1/2) for the direct allowed transition type and (3/2) for the direct forbidden values. Furthermore, this value is considered to be (2) for the indirect allowed transition type and 2/3 for the indirect forbidden type. The optical band gap magnitude can be determined by the perfect linear approximation in the $(\alpha h\nu)^{1/b}$ against $h\nu$ sketch and its extrapolation to $(\alpha h\nu)^{1/s} = 0$. For the films under examination, the perfect fitting is found for $b = 1/2$, revealing

that the transition is attributed to a direct allowed operation. Tauc's plot was employed for finding the optical band gap of the nanoporous sample and is shown in Fig. 4c. The value of the optical band gap for the nanoporous CAS is 3.93 eV.

The refractive index is significant for the electronic and opto-electronic properties, wherein the refractive index plays an important role in many devices. The refractive index value of the nanoporous CAS is determined with the following formula (Mansour et al. 2017b):

$$n = ((1+R)/(1-R)) + \sqrt{\left(4R/(1-R)^2\right) - k^2} \quad (5)$$

where k is the absorption index of the prepared nanoporous CAS that is estimated by utilizing the common formula,

$$k = \alpha\lambda/4\pi \quad (6)$$

The dispersion spectrum of the refractive index for CAS NPs is presented in Fig. 4d. As noted in the figure, the refractive index is approximately constant with increasing wavelength values and takes values between 1.7 and 1.9.

Antimicrobial activity of the synthesized nanoporous CAS disinfectant

Disc and well diffusion methods

The effects of public health and water-related outbreaks of diseases could be caused by the dangerous propagation of pathogenic microorganisms, these pathogens have an extreme resistant against antimicrobial materials (Köck et al. 2010). In past centuries, copper oxide is considering a good preserved of water, food, and therapeutic applications (Dollwet and Sorenson 1985; Karpanen et al. 2012), and CuO is broadly used for water management or for water delivery to consumers. Accordingly, the death and illness, caused by pathogens, are currently constrained in industrialized regions. CuO also has excellent biocidal properties with respect to bacteria, viruses, and fungi. Likewise, the small amounts of copper (adequate, efficient, and safe amounts) could be used to eliminate the growth of problematic microbes and realize bactericidal activity (Vincent et al. 2016).

According to Kim et al. (2006a), copper NPs (Cu NPs) deposited on the surface of spherical silica NPs result in a hybrid structure of the Cu-SiO_2 nanocomposite. SiO_2 NPs served as a substrate for the continuous deposition of copper. Nanoporous silica doped with copper nanocrystallites displayed antibacterial properties and had bactericidal effects on many pathogenic bacterial species (Singh et al. 2010). Therefore, the nanoporous CAS was synthesized via a green method to eradicate pathogenic microbes and to use as a disinfectant in drinking water and wastewater treatment.

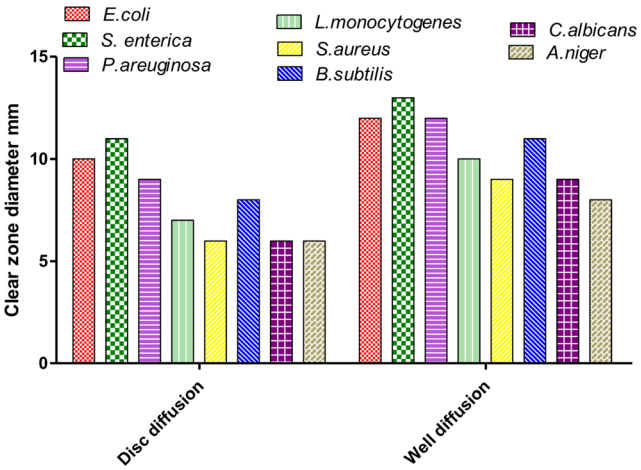

Fig. 5 Diameter of inhibition zones (mm) of nanoporous CAS disinfectant against tested microbial strains using both disc diffusion and well diffusion methods

The data presented in Fig. 5 display the diameter of the clear zones (mm) of the CAS disinfectant against the tested microbial strains using both disc diffusion and well diffusion methods. The nanoporous CAS disinfectant shows that the diameter of the clear zone ranged between 6 and 11 mm using the disc diffusion method and between 8 and 13 mm using the well diffusion method for all tested species. Essentially, the diameter of the clear zone differed among species, and the highest clear zone diameter was 11 and 13 for *S. enterica* using the disc diffusion and well diffusion methods, respectively, whereas the lowest diameter was 6 and 8 mm for *A. niger*, respectively.

In this study, the obtained results indicated that the diameter of the clear zone using the disc diffusion method is narrower than that using the well diffusion method. Moreover, the experimental results revealed that the tested Gram-negative bacterial species were more sensitive than Gram-positive species to CAS NPs. This result is due to the presence of copper (Cu) in the synthesized nanoporous structure, which can be used as a vigorous antimicrobial agent against problematic microbes that remain alive for just a few minutes on copper surfaces (Vincent et al. 2016). The obtained results were similar to the results of Kim et al. (2007), who assessed the bactericidal activities of nanoporous silicate by the disc diffusion assay against different types of pathogenic microbes, such as *S. aureus*, *P. aeruginosa*, *E. coli, C. albicans,* and *A. niger*. Additionally, sol–gel silica NPs doped with Cu are considered substitute antimicrobial agents for the currently used bactericidal agents; these nanoporous particles have various oxidation patterns of Cu. The dispersion of silica NPs in an aqueous solution is easy because of its hydrophilic properties, which increase the antimicrobial aspects of Cu. Likewise, the efficacy of the antimicrobial activity of a mixed-valence Cu system increases more accurate with Cu (0) and Cu (I) than with Cu (II) compounds (Young and

Santra 2014). In addition, Kim et al. (2006a) examined the antibacterial activity of nanoporous copper silicate (Cu-SiO_2) and verified that Cu-SiO_2 is a remarkable antibacterial agent. Many investigations have stated that the antimicrobial action of copper silicate resulted from its penetration of the dual layers of the membrane and the periplasmic space of Gram-negative and Gram-positive bacteria (Rice 2007; Kunz and Brook 2010).

The MICs of the nanoporous CAS disinfectant

To assess the antimicrobial action of the nanoporous CAS disinfectant, the MIC values of the studied disinfectant against the tested potential pathogenic microorganisms were determined at four different time intervals (5, 10, 20, 40 min). The initial counts of each tested pathogen are reported in Table 1. As shown in Fig. 6, the obtained results of the nanoporous CAS disinfectant with a short contact time (5 and 10 min) indicated a slight eradication effect against the tested pathogenic microbial strains. In contrast, the reduction percentage was increased with increasing contact time, which means that there is a positive relationship between the efficacy of the CAS disinfectant and the contact time. The influence of contact time on the reduction percentage achieved by the CAS disinfectant towards the tested microbes was unexpected; however, the reduction percentage significantly improved for all tested strains. The experimental results indicated that the MIC value of the nanoporous CAS disinfectant for the tested Gram-negative bacteria (*E. coli, S. enteric* and *P. aeruginosa*) was 100 mg/L within 20 min of contact time. In the case of Gram-positive bacteria (*S. aureus, L. monocytogenes,* and *E. faecalis*) and fungi (*C. albicans* and *A. niger*), these microbes persist for extensive time intervals up to 40 min. Accordingly, the MIC value of the CAS disinfectant was 100 mg/L within 40 min of contact time. These results are in agreement with those of Reyes-Jara et al. (2016) who revealed that Cu NPs had extreme antibacterial effects against *E. coli* and *S. aureus*. Likewise, the bactericidal properties of the metal NPs were examined against two Gram-negative (*E. coli* and *S. typhimurium*) and two Gram-positive (*S. aureus* and *L. monocytogenes*) bacteria. The antibacterial assay showed that these NPs displayed remarkable bacterial suppression (Gaballah et al. 2019).

The results shown in Table 1 revealed that the MIC values for Gram-negative bacteria were lower than those for the other tested microbes. In addition, the nanoporous CAS disinfectant removed all tested problematic microbes. In addition, the highest CAS disinfectant dosage (100 mg/L) should safely eradicate the studied microbial strains, meaning that it prevents the reproduction of all tested problematic pathogenic strains. As shown in Fig. 5 and Table 1, the reduction percentage reaches 100% for all the tested microbial strains. In addition, whole inactivation of microbial viable cells was achieved for all the studied strains using 100 mg/L of the CAS disinfectant. Table 1 reports the determined MIC values of the CAS disinfectants for the test strains as well as the corresponding reduction percentage.

Yoon et al. (2007) investigated the sensitivity of *B. subtilis* and *E. coli* against Ag and Cu NPs. They revealed that *B. subtilis* had the highest susceptibility to Cu NPs, whereas the reaction of Ag NPs with *E. coli* exhibited the lowest susceptibility. Furthermore, Usman et al. (2013) who evaluated the microbicidal action of chitosan NPs with Cu against many different types of infectious microbes, including *B. subtilis*, *P. aeruginosa*, methicillin-resistant *S. aureus*, *S. choleraesuis*, and *C. albicans,* and found that these NPs were more efficient in inactivating these microbes. Likewise, Ren et al. (Ren et al. 2009a) investigated the antibacterial properties of CuO NPs against *S. aureus* EMRSA-16 (epidemic methicillin-resistant *S. aureus*), methicillin-resistant *S. aureus*, *E. coli*, *P. aeruginosa*, and *Proteus* spp., as well as CuO NPs combined with polymers, and they proposed

Table 1 The initial cell counts of tested microbial strains and estimated MIC values of nanoporous CAS disinfectant

Tested potential microbial strains	Initial count (CFU/ml)	Nanoporous CAS disinfectant		
		MIC	Contact time	Removal %
E. coli	3.7×10^6	100 mg/L	20 min	100
Salmonella enterica	4.5×10^6	100 mg/L	20 min	100
Pseudomonas aeruginosa	2.9×10^6	100 mg/L	20 min	100
Staphylococcus aureus	6.3×10^6	100 mg/L	40 min	100
Listeria monocytogenes	4.1×10^6	100 mg/L	40 min	100
Enterococcus faecalis	1.7×10^6	100 mg/L	40 min	100
Candida albicans	3.2×10^6	100 mg/L	40 min	100
Aspergillus niger	5.2×10^6	100 mg/L	40 min	100

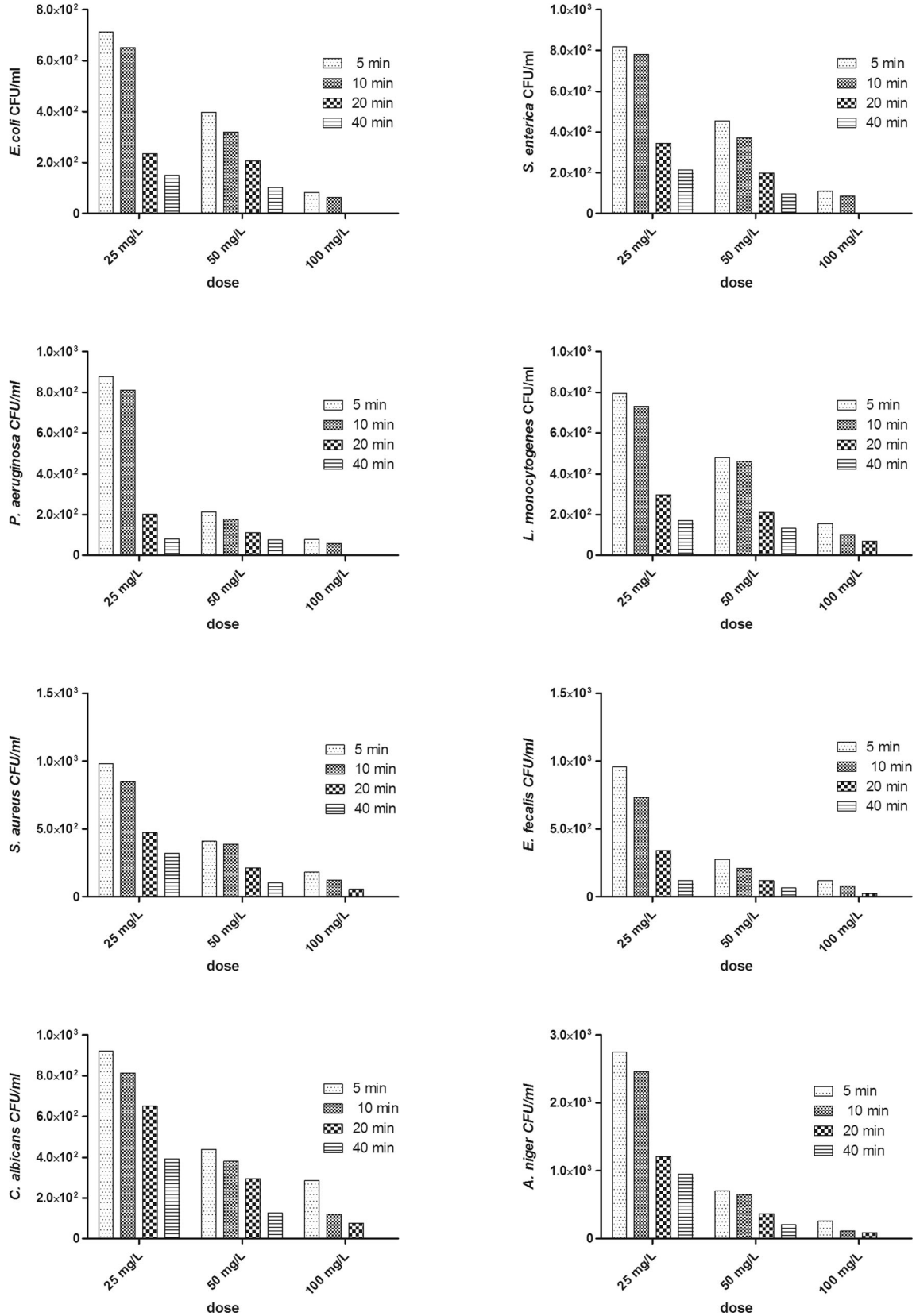

Fig. 6 Effect of three different doses of nanoporous CAS disinfectant on the inactivation of *E. coli, S. enterica, P. aeruginosa, S. aureus, L. monocytogenes, E. faecalis, C. albicans*, and *A. niger* at four various time intervals at room temperature (i.e., 26 ± 1 °C)

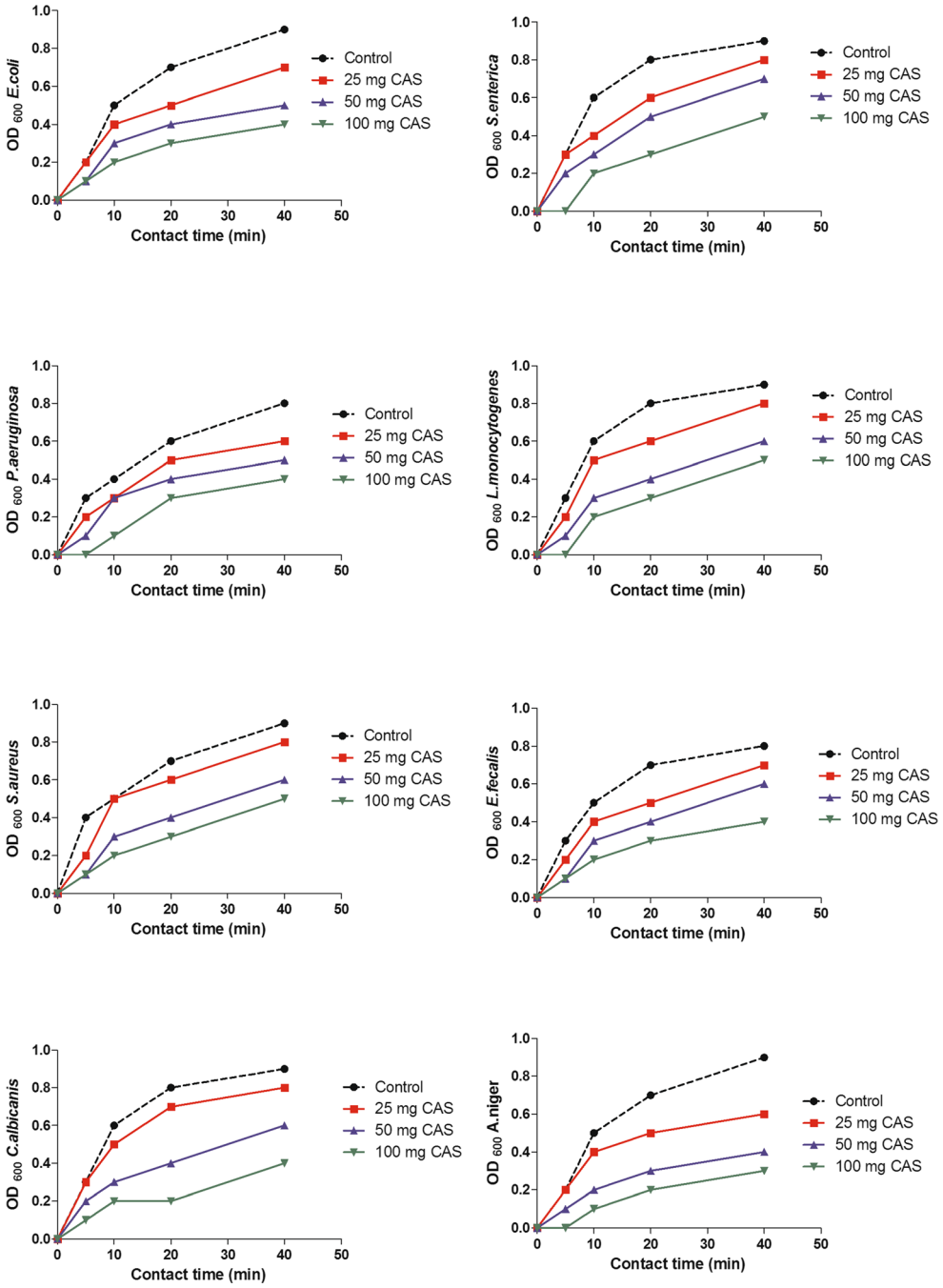

Fig. 7 Growth rate of *E. coli, S. enterica, P. aeruginosa, S. aureus, L. monocytogenes, E. faecalis, C. albicans*, and *A. niger* before and after exposure to different doses of nanoporous CAS disinfectant

that the release of ions may be necessary for optimum antimicrobial action. Ren et al. (2009b) established that the MIC of CuO NPs in relation to *P. aeruginosa* is ~ 5000 μg/mL. They also proposed that the release of copper ions into the limited atmosphere was needed for suppression of microbial activity and inhibition of bacterial reproduction. In addition, El Hotaby et al. (2017) found that the complete eradication of the Gram-positive bacteria, Gram-negative bacteria, and fungi was accomplished using an amount as low as 25 μg/mL of the prepared nanocomposite because of its biocompatibility.

For the bactericidal assessment, the results confirmed the antimicrobial action of the nanoporous CAS disinfectant against Gram-negative bacteria, Gram-positive bacteria, and fungi because the Cu NPs of the Cu-SiO_2 nanocomposite were well formed on the surface of the SiO_2 NPs without aggregation of the Cu NPs, and they had a large surface area. These results agree with those of Bagchi et al. (2013), who indicated that Cu NPs had a high constancy in the atmosphere and remarkable microbiological activity against many bacterial species, such as *E. coli*, *S. aureus*, *P. aeruginosa,*

Table 2 The densities of microbial cells in three water samples before treatment with nanoporous CAS disinfectant

Tested pathogenic microbes	Unit	Type of water samples		
		Raw wastewater	Raw Nile water	Injected drinking water
E. coli	CFU/ml	5.2×10^6	3.6×10^3	2.8×10^6
S. enterica	CFU/ml	2.9×10^6	2.3×10^3	1.3×10^6
P. aeruginosa	CFU/ml	1.7×10^6	4.3×10^3	4.2×10^6
S. aureus	CFU/ml	8.4×10^5	5.7×10^2	3.1×10^6
L. monocytogenes	CFU/ml	4.7×10^5	2.6×10^2	5.2×10^6
E. faecalis	CFU/ml	3.1×10^5	1.5×10^3	4.7×10^6
C. albicans	CFU/ml	2.9×10^6	3.7×10^3	3.6×10^6
A. niger	CFU/ml	6.3×10^5	4.2×10^2	2.9×10^6

and *E. faecalis*, resulting in a decrease in the bacterial numbers of more than 90% within 12 h. In addition, Mahapatra et al. (2008) assessed the bactericidal properties of CuO NPs against some Gram-negative bacterial species, including *S. paratyphi, P. aeruginosa, Klebsiella apneumoniae*, and *Shigella* strains. In accordance with their results, these NPs had efficacious antibacterial activity against these bacteria. The investigators also supposed that the NPs were highly capable of penetrating into the outer layer of bacterial cells and then destroying significant bacterial enzymes, causing serious issues that led to the death of the bacterial cells. Moreover, Bogdanović et al. (2014) studied the biocidal action of Cu NPs against some infectious microbes that are of concern for human health (*E. coli*, *S. aureus*, and *C. albicans*). Based on their findings, it was revealed that these Cu NPs displayed remarkable biocidal activity against various types of infectious microorganisms (*E. coli*, *S. aureus*, and *C. albicans*).

The antimicrobial activity of SiO_2 is very large at the nanoparticle size due to the expansion of the surface area (Bogdanović et al. 2014). However, Bogdanović et al. (2014) revealed that Si NPs could inhibit bacteria that have a good ability to adhere to solid surfaces to form biofilms. The mixture of Si NPs with other bactericidal NPs, such as Ag or Cu, has been extensively considered. Likewise, Kim et al. (2006b)indicated that the Cu/SiO_2 nanocomposite was examined by disc diffusion methods and had remarkable antibacterial properties.

In conclusion, the results showed that the tested nanoporous CAS nanocrystallites had vigorous antimicrobial properties against multiple problematic infectious microbial strains. These results are compatible with those of Esteban-Cubillo et al. (2006) who confirmed that nanoporous Cu NPs deposited on magnesium silicate are potent bactericidal agents against *S. aureus* and *E. coli* bacteria.

Growth rate of each tested microbial pathogen

Figure 7 shows the growth rate of each tested pathogen. These problematic pathogens were individually subjected to three doses of the nanoporous CAS disinfectant (25, 50, and 100 mg). The growth rates of all tested potential microbial pathogenic strains decreased gradually after exposure to all doses of the studied nanoporous CAS disinfectants. These results are in accordance with the results of Maniprasad and Santra (2012) who examined the antibacterial efficacy of nanocrystalline Cu-silica NPs against *E. coli* and *B. subtilis* and obtained highly efficient bactericidal activity with formidable bioavailability and a decreasing rate of bacterial proliferation.

Based on this hypothesis, the growth rate of microbial pathogens could be prohibited by Cu NPs. Regarding the nanoporous CAS mechanism of action, the interactions between CuO NP and bacterial cell consider as a consequence of conflicting electrical charges lead to a reduction reaction in the bacterial cell wall, which affected the attachment and bioactivity due to the electrostatic charges (Raffi et al. 2010). In the case of Gram-negative bacteria, the cell wall is mainly composed of lipopolysaccharides and carboxylates, and sulfhydryl groups, which cause the negative charge, play an essential role as membrane active sites (Navarro et al. 2008). The destruction of double-stranded DNA, the denaturation of protein, and the change in the membrane integrity can be caused by the interaction of these groups in the bacterial cell wall with CuO NPs (Grass et al. 2011; Chaturvedi and Henderson 2014).

Toxicity results

The use of safe substitutes and effective disinfectants in water is required for public health. The toxin concentrations were measured in aqueous solutions of the nanoporous CAS disinfectant and treated water using a

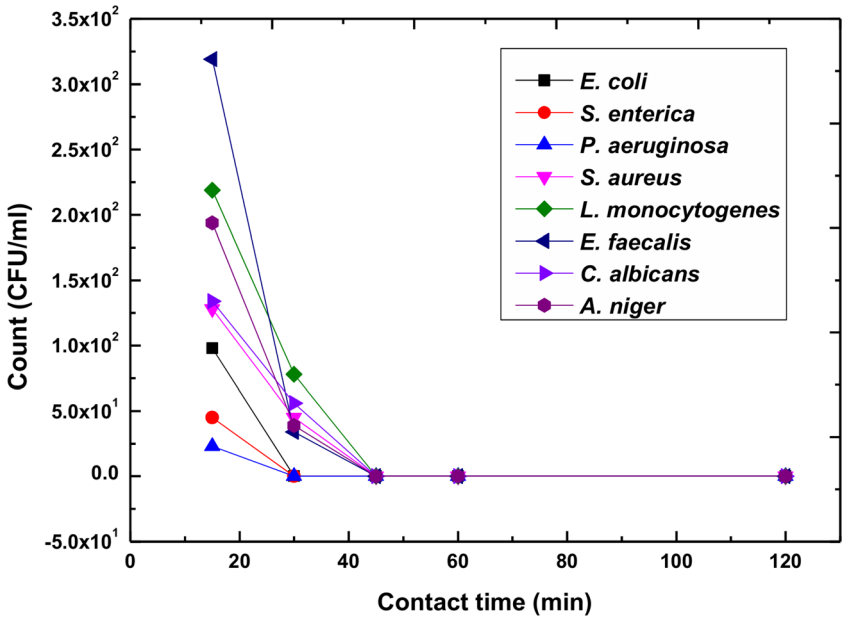

Fig. 8 Disinfection of raw Nile water by 100 mg/L of nanoporous CAS disinfectant with different time intervals

Microtox Analyzer 500 Luminometer. The aqueous solutions of the synthesized disinfectant were incubated for 10 min and then exposed to heavy light for the same amount of time as a control sample. The results indicated that there was no variance between the test and control samples. It is clear that the *Vibrio fischeri* level in all samples was steady. The Microtox EC_{50} measurements of the CAS disinfectant were 450 mg/L (> 100 mg/L), indicating that there is no toxicity of the studied disinfectant, and this material could also be safely used for water treatment. These results are in agreement with the results of Flokstra et al. (2008). In addition, the cytotoxicity assay of the nanoporous CAS disinfectant showed that it was nontoxic against the Hep-2 cell line. Clearly, copper is an effective agent with fairly low toxicity to warm-blooded animals (Elsaesser and Howard 2012). Ren et al. (2009a) established that Cu NPs were safe and that they did not have any toxicity effect on the HeLa cell line. The toxicity and environmental fate of NPs are eventual concerns for the selection of disinfectants for water purification. Apparently, the use of nanostructure materials is superior when comparing with other approaches for water purification, but the current awareness of ecological protection and the transport and toxicity of NPs must be considered (Gupta et al. 2018).

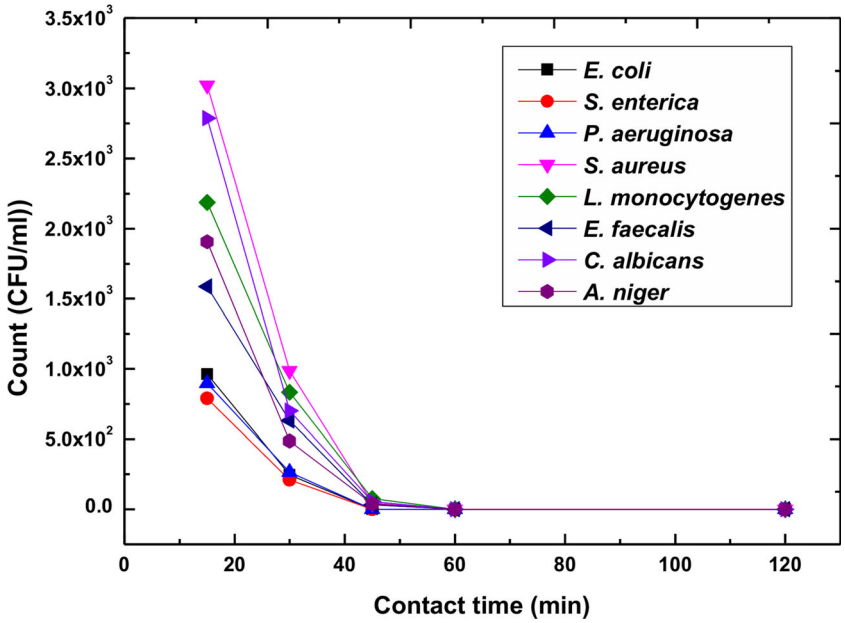

Fig. 9 Disinfection of inoculated drinking water by 100 mg/L of nanoporous CAS disinfectant with different time intervals

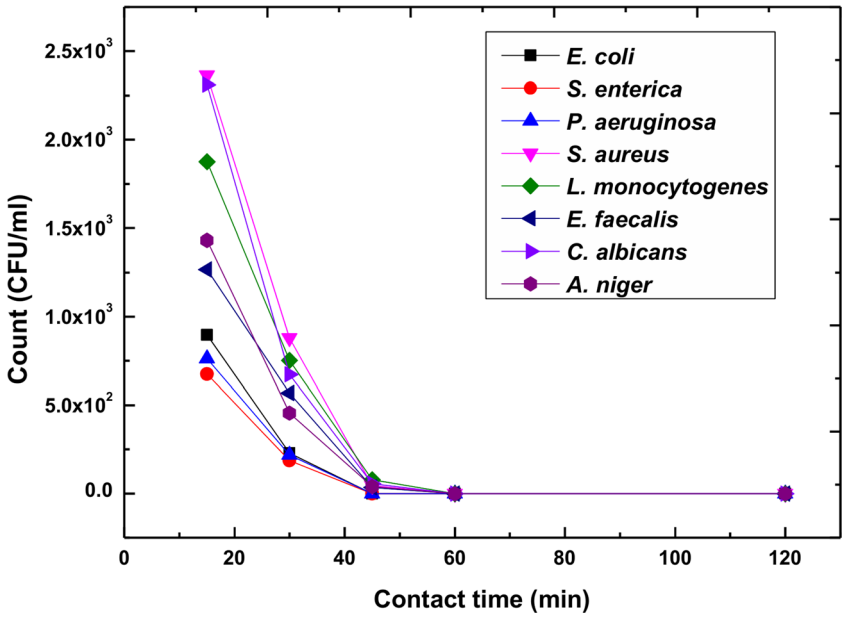

Fig. 10 Disinfection of raw domestic wastewater by 100 mg/L of nanoporous CAS disinfectant with different time intervals

Usage of the synthesized CAS disinfectant in water and wastewater purification

The broad spectrum of organic and inorganic pollutants in water is considered one of the most hazardous problems as a result of rapid advancement and population growth. The destroying of the environment and occurring of problematic microbes caused by dangerous pollutants are threat issues for researchers that have investigated to eliminate these pollutants from water (Sharma and Pant 2009). Nanotechnology provides the opportunity for the effective removal of pollutants and microbial contaminants. Furthermore, NPs, nanocomposites and nanopowders have been used for the removal of chemical and organic constituents from water and wastewater (Tiwari et al. 2008).

Synthesized nanoporous CAS disinfectants have been determined to be well-designed nanomaterials for the deactivation of diverse kinds of problematic microorganisms during water purification. Raw Nile water, inoculated drinking water, and raw wastewater samples were used to assess the effectiveness of the CAS disinfectant for water and wastewater disinfection. Table 2 reports the microbiological examination results of all tested water samples for the determination of the initial counts of all tested microbes in the studied water samples. The concentration of the CAS disinfectant (100 mg/L) was used to sanitize three different types of water (50 mL of raw Nile water, 50 mL of inoculated drinking water, and 50 mL of raw wastewater). The results of the treatment of raw water, inoculated water, and raw wastewater samples using the nanoporous CAS disinfectant as a function of time are illustrated in Figs. 8, 9, and 10, respectively.

As shown in Fig. 8, the dosage of disinfectant (100 mg/L) was suitable for the whole inactivation of *E. coli*, *P. aeruginosa*, and *S. enterica* within 30 min, while *S. aureus*, *L. monocytogenes, C. albicans*, and *A. niger* took 45 min to produce the same effect. In the case of the inoculated drinking water and raw wastewater samples, the results illustrated graphically in Figs. 9 and 10 show that the nanoporous CAS disinfectant (100 mg/L) was able to fully remove all tested Gram-negative bacterial cells after 45 min, while Gram-positive and fungal cells needed more time (60 min) for complete eradication. These results are compatible with results by Elwakeel et al. (2018), who discovered that the studied Ag NPs could eradicate some infectious microbes present in water and wastewater. The higher dosage of disinfectant (0.5 mg/mL) was used to purify surface and wastewater samples at different contact times.

The harmful effect on water quality might result in a severe threat to the lifecycle due to the presence of pathogenic microbes. The synthesis and usage of promising methods for preventing the contamination of water have become essential subjects (Gupta et al. 2018). The synthesized novel amine-functionalized magnetite Fe_3O_4–SiO_2–NH_2 NPs were used to eradicate infectious microbial species (Zhan et al. 2014). Likewise, the elimination efficiency percentage of Fe_3O_4–SiO_2–NH_2 NPs to prohibit problematic pathogenic bacteria reached 97.39. Furthermore, the modified magnetic iron oxide NPs with antibacterial properties are much more efficient than other NPs against bacteria (Jin et al. 2015). In addition, these synthesized magnetic NPs not only potentially catch *B. subtilis*, as an example of Gram-positive bacteria, and *E. coli*, as an example of Gram-negative bacteria, from water but also deactivate bacterial cells with extreme efficiency up to 99% within 60 min (Jin et al. 2015). Similarly, Dankovich and

Smith (2014) discovered that Cu NPs could be used as drinking water purifiers. Cu NPs could decrease *E. coli* bacterial cells by approximately log 8.8 CFU/mL.

Conclusion

Clustered nanoporous CAS is synthesized using the green sol–gel method from the facile and excellently formed aluminum and copper sols, which are prepared and then mixed with acidic silica sol. The transformation of the CAS sol viscosity with the aging process and with drying at 200 °C suggests the substantial formation of nanoclustered long-chain structures during the sol–gel polymerization and densification processes. The XRD results show that the synthesized sample is cubic CAS. Both HR-TEM and FE-SEM reveal the formation of an ordered CAS nanoporous material composed of NPs with dense spherical shapes. The UV-Vis absorption spectra reveal the high transparency of the nanoporous CAS, with a high band gap energy (~ 3.93 eV) and a refractive index in the range of 1.7–1.9. The MIC of the nanoporous CAS disinfectant against *E. coli*, *S. enterica*, and *P. aeruginosa* is 100 mg/L within 20 min of contact time, and the MIC of the CAS disinfectant is 100 mg/L within 40 min of contact time for the other strains. The efficacy of antimicrobial action (100%) is reached within 20 to 40 min against all pathogens. Herein, the CAS disinfectant is safe for humans without any toxicity. Nanoporous CAS disinfectants will provide a promising, affordable, convenient, and effective approach to eradicate problematic waterborne pathogens in water disinfection.

Funding information The authors would like to thank the National Research Centre (NRC), Egypt, for their financial support and providing the equipment required.

Compliance with ethical standards

Conflict of interests The authors declare that they have no conflict of interest.

References

Alghamdi H, Dakhane A, Alum A, Abbaszadegan M, Mobasher B, Neithalath N (2018) Synthesis and characterization of economical, multi-functional porous ceramics based on abundant aluminosilicates. Mater Des 152:10–21. https://doi.org/10.1016/j.matdes.2018.04.060

American Public Health Association, American Water Works Association, Water Environment Federation (2012) Standard methods for the examination of water and wastewater, 22nd edn. Am Public Heal Assoc, Washingto, DC, USA ISBN 9780875532356

Bagchi B, Kar S, Dey SK, Bhandary S, Roy D, Mukhopadhyay TK, Das S, Nandy P (2013) In situ synthesis and antibacterial activity of copper nanoparticle loaded natural montmorillonite clay based on contact inhibition and ion release. Colloids Surf B Biointerfaces. 108:358–365. https://doi.org/10.1016/j.colsurfb.2013.03.019

Bian N, Mayanovic RA, Benamara M (2018) Synthesis and characterization of Co3O4-MnxCo3-xO4Core-Shell nanoparticles. MRS Advances, In

Bogdanović U, Lazić V, Vodnik V, Budimir M, Marković Z, Dimitrijević S (2014) Copper nanoparticles with high antimicrobial activity. Mater Lett 128:75–78. https://doi.org/10.1016/j.matlet.2014.04.106

Chaturvedi KS, Henderson JP (2014) Pathogenic adaptations to host-derived antibacterial copper. Front Cell Infect Microbiol 4. https://doi.org/10.3389/fcimb.2014.00003

Craun MF, Craun GF, Calderon RL, Beach MJ (2006) Waterborne outbreaks reported in the United States. J Water Health 4:19–30. https://doi.org/10.2166/wh.2006.016

Dankovich TA, Smith JA (2014) Incorporation of copper nanoparticles into paper for point-of-use water purification. Water Res 63:245–251. https://doi.org/10.1016/j.watres.2014.06.022

De Velasco-Maldonado PS, Hernández-Montoya V, Montes-Morán MA et al (2018) Surface modification of a natural zeolite by treatment with cold oxygen plasma: characterization and application in water treatment. Appl Surf Sci 434:1193–1199. https://doi.org/10.1016/j.apsusc.2017.11.023

Dollwet HHA, Sorenson JRJ (1985) Historic uses of copper compounds in medicine. Trace Elem Med 2:80–87

El Hotaby W, Sherif HHA, Hemdan BA et al (2017) Assessment of in situ-prepared polyvinylpyrrolidone-silver nanocomposite for antimicrobial applications. Acta Phys Pol A 131:1554–1560. https://doi.org/10.12693/APhysPolA.131.1554

Elith J, Leathwick JR (2009) Species distribution models: ecological explanation and prediction across space and time. Annu Rev Ecol Evol Syst 40:677–697. https://doi.org/10.1146/annurev.ecolsys.110308.120159

El Nahrawy AM (2015) Structural studies of sol gel prepared nanocrystalline silica zinc titanate ceramic. Intr J Advanc Engin Technol Computer Sci 2:15–18

El Nahrawy A, AbouHammad AB (2016) A facile co-gelation sol gel route to synthesize cao: P2o5: Sio2 xerogel embedded in chitosan nanocomposite for bioapplications. Int J Pharm Tech Res 9:16–21

El Nahrawy AM, Ali AI (2014) Influence of reaction conditions on sol-gel process producing SiO2 and SiO2 -P2O5 gel and glass. J Glas Ceram 04:42–47. https://doi.org/10.4236/njgc.2014.42006

El Nahrawy AM, Kim YS, Ali AI (2016) Synthesis of hybrid chitosan/calcium aluminosilicate using a sol-gel method for optical applications. J Alloys Compd 676:432–439. https://doi.org/10.1016/j.jallcom.2016.03.210

El Nahrawy AM, Moez AA, Saad AM (2018) Sol-gel preparation and spectroscopic properties of modified sodium silicate /Tartrazine dye nanocomposite. Silicon 10:2117–2122. https://doi.org/10.1007/s12633-017-9740-9

Elsaesser A, Howard CV (2012) Toxicology of nanoparticles. Adv Drug Deliv Rev 64:129–137

Elwakeel KZ, El-Liethy MA, Ahmed MS et al (2018) Facile synthesis of magnetic disinfectant immobilized with silver ions for water pathogenic microorganism's deactivation. Environ Sci Pollut Res 25:22797–22809. https://doi.org/10.1007/s11356-018-2071-6

Esteban-Cubillo A, Pecharromán C, Aguilar E, et al (2006) Antibacterial activity of copper monodispersed nanoparticles into sepiolite. In: J Materials Sci 41(16):5208–5212. https://doi.org/10.1007/s10853-006-0432-x

Farag AAM, Mansour AM, Ammar AH, Rafea MA, Farid AM (2012) Electrical conductivity, dielectric properties and optical absorption of organic based nanocrystalline sodium copper chlorophyllin for

photodiode application. J Alloys Compd 513:404–413. https://doi.org/10.1016/j.jallcom.2011.10.058

Fenwick A (2006) Waterborne infectious diseases - could they be consigned to history?. Science 313(5790):1077–1081. https://doi.org/10.1126/science.1127184

Flokstra BR, Van Aken B, Schnoor JL (2008) Microtox® toxicity test: detoxification of TNT and RDX contaminated solutions by poplar tissue cultures. Chemosphere 71:1970–1976. https://doi.org/10.1016/j.chemosphere.2007.12.020

Ford TE (1999) Microbiological safety of drinking water: United States and global perspectives. Environ Health Perspect 107:191. https://doi.org/10.2307/3434483

Gaballah ST, El-Nazer HA, Abdel-Monem RA et al (2019) Synthesis of novel chitosan-PVC conjugates encompassing Ag nanoparticles as antibacterial polymers for biomedical applications. Int J Biol Macromol 121:707–717. https://doi.org/10.1016/j.ijbiomac.2018.10.085

Grass G, Rensing C, Solioz M (2011) Metallic copper as an antimicrobial surface. Appl Environ Microbiol 77:1541–1547

Guo X, Li W, Nakanishi K, Kanamori K, Zhu Y, Yang H (2013) Preparation of mullite monoliths with well-defined macropores and mesostructured skeletons via the sol-gel process accompanied by phase separation. J Eur Ceram Soc 33:1967–1974. https://doi.org/10.1016/j.jeurceramsoc.2013.02.018

Gupta N, Pant P, Gupta C, Goel P, Jain A, Anand S, Pundir A (2018) Engineered magnetic nanoparticles as efficient sorbents for wastewater treatment: a review. Mater Res Innov 22:434–450. https://doi.org/10.1080/14328917.2017.1334846

Hao OJ, Lin C-F, Fu-Tien J, Chien-Jen S (1995) A review of Microtox test and its applications. Toxicol Environ Chem 52:57–76

Hellard ME, Sinclair MI, Forbes AB, Fairley CK (2001) A randomized, blinded, controlled trial investigating the gastrointestinal health effects of drinking water quality. Environ Health Perspect 109:773–778. https://doi.org/10.1289/ehp.01109773

Hisatomi T, Kubota J, Domen K (2014) Recent advances in semiconductors for photocatalytic and photoelectrochemical water splitting. Chem Soc Rev 43:7520–7535

Hongquan Z, Yuhua Y, Youfa W, Shipu L (2003) Morphology and formation mechanism of hydroxyapatite whiskers from moderately acid solution. Mater Res 6:111–115

Jamil TS, Mansor ES, Azab El-Liethy M (2015) Photocatalytic inactivation of E. Coli using nano-size bismuth oxyiodide photocatalysts under visible light. J Environ Chem Eng 3:2463–2471. https://doi.org/10.1016/j.jece.2015.09.017

Jin R, Yang Y, Xing Y, Chen L, Song S, Jin R (2014) Facile synthesis and properties of hierarchical double-walled copper silicate hollow nanofibers assembled by nanotubes. ACS Nano 8:3664–3670. https://doi.org/10.1021/nn500275d

Jin Y, Deng J, Liang J, Shan C, Tong M (2015) Efficient bacteria capture and inactivation by cetyltrimethylammonium bromide modified magnetic nanoparticles. Colloids Surf B Biointerfaces 136:659–665. https://doi.org/10.1016/j.colsurfb.2015.10.009

Jones GL (1973) Bacterial growth kinetics: measurement and significance in the activated-sludge process. Water Res 7:1475–1492. https://doi.org/10.1016/0043-1354(73)90120-6

Kajihara K (2013) Recent advances in sol-gel synthesis of monolithic silica and silica-based glasses. J Asian Ceram Soc 1(2):121–133. https://doi.org/10.1016/j.jascer.2013.04.002Get

Karpanen TJ, Casey AL, Lambert PA, Cookson BD, Nightingale P, Miruszenko L, Elliott TSJ (2012) The antimicrobial efficacy of copper alloy furnishing in the clinical environment: a crossover study. Infect Control Hosp Epidemiol 33:3–9. https://doi.org/10.1086/663644

Kaur K, Singh KJ, Anand V, Bhatia G, Singh S, Kaur H, Arora DS (2016) Magnesium and silver doped CaO–Na2O–SiO2–P2O5 bioceramic nanoparticles as implant materials. Ceram Int 42:12651–12662. https://doi.org/10.1016/j.ceramint.2016.05.001

Kaur P, Singh KJ, Yadav AK, Sood H, Kaur S, Kaur R, Arora DS, Kaur S (2018) Preliminary investigation of the effect of doping of copper oxide in CaO-SiO2-P2O5-MgO bioactive composition for bone repair applications. Mater Sci Eng C 83:177–186. https://doi.org/10.1016/j.msec.2017.09.006

Khezerlou A, Alizadeh-Sani M, Azizi-Lalabadi M, Ehsani A (2018) Nanoparticles and their antimicrobial properties against pathogens including bacteria, fungi, parasites and viruses. Microb Pathog 123:505–526. https://doi.org/10.1016/j.micpath.2018.08.008

Kim YH, Lee DK, Cha HG, Kim CW, Kang YC, Kang YS (2006a) Preparation and characterization of the antibacterial Cu nanoparticle formed on the surface of SiO2 nanoparticles. J Phys Chem B 110:24923–24928. https://doi.org/10.1021/jp0656779

Kim YH, Lee DK, Cha HG, Kim CW, Kang YC, Kang YS (2006b) Preparation and characterization of the antibacterial Cu nanoparticle formed on the surface of SiO2 nanoparticles. J Phys Chem B 110:24923–24928. https://doi.org/10.1021/jp0656779

Kim YH, Lee DK, Cha HG, Kim CW, Kang YS (2007) Synthesis and characterization of antibacterial Ag - SiO2nanocomposite. J Phys Chem C 111:3629–3635. https://doi.org/10.1021/jp068302w

Köck R, Becker K, Cookson B, et al (2010) Methicillin-resistant staphylococcus aureus (MRSA): burden of disease and control challenges in Europe. Eurosurveillance 15(41):19688. https://doi.org/10.2807/ese.15.41.19688-en

Kunz AN, Brook I (2010) Emerging resistant gram-negative aerobic bacilli in hospital-acquired infections. Chemotherapy 56:492–500. https://doi.org/10.1159/000321018

Mahapatra O, Bhagat M, Gopalakrishnan C, Arunachalam KD (2008) Ultrafine dispersed CuO nanoparticles and their antibacterial activity. J Exp Nanosci 3:185–193. https://doi.org/10.1080/17458080802395460

Maniprasad P, Santra S (2012) Novel copper (cu) loaded core-shell silica nanoparticles with improved cu bioavailability: synthesis, characterization and study of antibacterial properties. J Biomed Nanotechnol 8:558–566. https://doi.org/10.1166/jbn.2012.1423

Mansour AM, El-Menyawy EM, Mahmoud GM et al (2017a) Structural, optical and galvanomagnetic properties of nanocrystalline se 51.43 in 44.67 Pb 3.9 thin films. Mater Res Express 4:115903. https://doi.org/10.1088/2053-1591/aa95ee

Mansour AM, El-Taweel FMAA, Abu El-Enein RANN, El-Menyawy EM (2017b) Structural, optical, electrical and photoelectrical properties of 2-Amino-4-(5-bromothiophen-2-yl)-5,6-dihydro-6-methyl-5-oxo-4H-pyrano[3,2-c] quinoline-3-carbonitrile films. J Electron Mater 46:1–8. https://doi.org/10.1007/s11664-017-5739-7

Navarro E, Baun A, Behra R, Hartmann NB, Filser J, Miao AJ, Quigg A, Santschi PH, Sigg L (2008) Environmental behavior and ecotoxicity of engineered nanoparticles to algae, plants, and fungi. Ecotoxicology 17:372–386

Øye G, Glomm WR, Vrålstad T, Volden S, Magnusson H, Stöcker M, Sjöblom J (2006) Synthesis, functionalisation and characterisation of mesoporous materials and sol-gel glasses for applications in catalysis, adsorption and photonics. Adv Colloid Interf Sci 123-126:17–32

PA W (2015) CLSI Methods for dilution antimicrobial susceptibility tests for bacteria that grow aerobically; approved standard—tenth edition. CLSI document M07-A10. Clinical and Laboratory Standards Institute, Wayne, PA

Pandey PK, Kass PH, Soupir ML, et al (2014) Contamination of water resources by pathogenic bacteria. AMB Express 4:51. https://doi.org/10.1186/s13568-014-0051-x

Raffi M, Mehrwan S, Bhatti TM, Akhter JI, Hameed A, Yawar W, ul Hasan MM (2010) Investigations into the antibacterial behavior of copper nanoparticles against Escherichia coli. Ann Microbiol 60:75–80. https://doi.org/10.1007/s13213-010-0015-6

Ren G, Hu D, Cheng EWC, Vargas-Reus MA, Reip P, Allaker RP (2009a) Characterisation of copper oxide nanoparticles for antimicrobial applications. Int J Antimicrob Agents 33:587–590. https://doi.org/10.1016/j.ijantimicag.2008.12.004

Ren G, Hu D, Cheng EWC, Vargas-Reus MA, Reip P, Allaker RP (2009b) Characterisation of copper oxide nanoparticles for antimicrobial applications. Int J Antimicrob Agents 33:587–590. https://doi.org/10.1016/j.ijantimicag.2008.12.004

Reyes-Jara A, Cordero N, Aguirre J, Troncoso M, Figueroa G (2016) Antibacterial effect of copper on microorganisms isolated from bovine mastitis. Front Microbiol 7:1–10. https://doi.org/10.3389/fmicb.2016.00626

Reynolds KA, Mena KD, Gerba CP (2008) Risk of waterborne illness via drinking water in the United States. Rev Environ Contam Toxicol 192:117–158. https://doi.org/10.1007/978-0-387-71724-1_4

Rice LB (2007) Emerging issues in the management of infections caused by multidrug-resistant gram-negative bacteria. Cleve Clin J Med 74: S12. https://doi.org/10.3949/ccjm.74.Suppl_4.S12

Sedlak DL, Von Gunten U (2011) The chlorine dilemma. Science 331(6013):42–43. https://doi.org/10.1126/science

Sharma RK, Pant P (2009) Preconcentration and determination of trace metal ions from aqueous samples by newly developed gallic acid modified Amberlite XAD-16 chelating resin. J Hazard Mater 163: 295–301. https://doi.org/10.1016/j.jhazmat.2008.06.120

Simões M, Simões LC, Vieira MJ (2010) A review of current and emergent biofilm control strategies. LWT - Food Sci Technol 43:573–583

Singh A, Krishna V, Angerhofer A, Do B, MacDonald G, Moudgil B (2010) Copper coated silica nanoparticles for odor removal. Langmuir 26:15837–15844. https://doi.org/10.1021/la100793u

Tiwari DK, Behari J, Sen P (2008) Application of nanoparticles in waste water treatment. Carbon Nanotub 3:417–433. https://doi.org/10.1016/j.matchemphys.2009.10.034

Tripathi VS, Kandimalla VB, Ju H (2006) Preparation of ormosil and its applications in the immobilizing biomolecules. Sensors Actuators B Chem 114:1071–1082

Trojanowicz M, Bojanowska-Czajka A, Bartosiewicz I, Kulisa K (2018) Advanced oxidation/reduction processes treatment for aqueous perfluorooctanoate (PFOA) and perfluorooctanesulfonate (PFOS) – a review of recent advances. Chem Eng J 336:170–199

UNCF (2014) The State of the World's Children 2014 -Every Child Counts.United Nations Children's Fund 2014.

United States Environmental Protection Agency (2017) Clean Water Act Section 303(d): Impaired Waters and Total Maximum Daily Loads (TMDLs). In: United States Environ. Prot. Agency

Usman MS, Zowalaty ME, El Shameli K et al (2013) Synthesis, characterization, and antimicrobial properties of copper nanoparticles. Int J Nanomedicine 8:4467–4479

Vincent M, Hartemann P, Engels-Deutsch M (2016) Antimicrobial applications of copper. Int J Hyg Environ Health 219:585–591. https://doi.org/10.1016/j.ijheh.2016.06.003

Wang Y, Lin F, Shang B, Peng B, Deng Z (2018) Self-template synthesis of nickel silicate and nickel silicate/nickel composite nanotubes and their applications in wastewater treatment. J Colloid Interface Sci 522:191–199. https://doi.org/10.1016/j.jcis.2018.03.044

WHO (2012) Good health adds life to years - global brief for world health day 2012. World Heal Organ. https://doi.org/10.1017/CBO9781107415324.004

WHO (2014) GLASS 2014 Report. Investing in water and sanitation: increasing access, reducing inequalities - UN-water global analysis and assessment of sanitation and drinking water. World Health Organization, Geneva

Yoon KY, Hoon Byeon J, Park JH, Hwang J (2007) Susceptibility constants of Escherichia coli and Bacillus subtilis to silver and copper nanoparticles. Sci Total Environ 373:572–575. https://doi.org/10.1016/j.scitotenv.2006.11.007

Young M, Santra S (2014) Copper (Cu)-silica nanocomposite containing valence-engineered Cu: a new strategy for improving the antimicrobial efficacy of cu biocides. J Agric Food Chem 62:6043–6052. https://doi.org/10.1021/jf502350w

Youssef AM, El-Nahrawy AM, Abou Hammad AB (2017) Sol-gel synthesis and characterizations of hybrid chitosan-PEG/calcium silicate nanocomposite modified with ZnO-NPs and (E102) for optical and antibacterial applications. Int J Biol Macromol 97:561–567. https://doi.org/10.1016/j.ijbiomac.2017.01.059

Zazouli MA, Kalankesh LR (2017) Removal of precursors and disinfection byproducts (DBPs) by membrane filtration from water; a review. J Environ Heal Sci Eng 15(1):25. https://doi.org/10.1186/s40201-017-0285-z

Zhan S, Yang Y, Shen Z, Shan J, Li Y, Yang S, Zhu D (2014) Efficient removal of pathogenic bacteria and viruses by multifunctional amine-modified magnetic nanoparticles. J Hazard Mater 274:115–123. https://doi.org/10.1016/j.jhazmat.2014.03.067

Zhan G, Yec CC, Zeng HC (2015) Mesoporous bubble-like manganese silicate as a versatile platform for design and synthesis of nanostructured catalysts. Chem - A Eur J 21:1882–1887. https://doi.org/10.1002/chem.201405697

Zhang S, Fu R, Dingcai W et al (2004) Preparation and characterization of antibacterial silver-dispersed activated carbon aerogels. Carbon N Y 42:3209–3216. https://doi.org/10.1016/j.carbon.2004.08.004